Available online at www.sciencedirect.com
ScienceDirect
Biochimica et Biophysica Acta 1774 (2007) 1148–1155
Biochimica et Biophysica Acta
BBA
www.elsevier.com/locate/bbapap

The connection between metal ion affinity and ligand affinity in integrin I domains

Thomas Vorup-Jensen [a,c,1], Travis T. Waldron [a,1], Nathan Astrof [a], Motomu Shimaoka [b], Timothy A. Springer [a,*]

[a] CBR Institute for Biomedical Research and Department of Pathology, Harvard Medical School, 200 Longwood Avenue, Boston, MA 02115, USA
[b] CBR Institute for Biomedical Research and Department of Anesthesia, Harvard Medical School, 200 Longwood Avenue, Boston, MA 02115, USA
[c] Biophysical Immunology Laboratory, Institute for Medical Microbiology and Immunology, University of Aarhus, DK-8000 Aarhus C, Denmark

Received 28 March 2007; received in revised form 20 June 2007; accepted 21 June 2007
Available online 12 July 2007

Abstract

Integrins are cell-surface heterodimeric proteins that mediate cell–cell, cell–matrix, and cell–pathogen interactions. Half of the known integrin α subunits contain inserted domains (I domains) that coordinate ligand through a metal ion. Although the importance of conformational changes within isolated I domains in regulating ligand binding has been reported, the relationship between metal ion binding affinity and ligand binding affinity has not been elucidated. Metal and ligand binding by several I domain mutants that are stabilized in different conformations are investigated using isothermal titration calorimetry and surface plasmon resonance studies. This work suggests an inverse relationship between metal ion affinity and ligand binding affinity (i.e. constructs with a high affinity for ligand exhibit a low affinity for metal). This trend is discussed in the context of structural studies to provide an understanding of interplay between metal ion binding and ligand affinities and conformational changes.

Keywords: Integrin; Metal ion; LFA-1; ICAM-1; Isothermal calorimetry; Surface plasmon resonance

1. Introduction

Integrins are cell-surface heterodimeric proteins (consisting of an alpha chain and a beta chain) that mediate cell–cell, cell–matrix, and cell–pathogen interactions. They are involved in a wide range of physiological processes including inflammation, cell migration, and wound healing. Half of the eighteen α subunits that have been discovered contain an inserted (I) domain (also known as a von Willebrand Factor A domain). When present in the integrin, the I domain is the major ligand binding site. Integrin I domains are 180–190 amino acids in length and adopt a Rossmann-like fold with seven α-helices surrounding a central, six-stranded β-sheet [1]. Furthermore, I domains contain a Mg^{2+} ion binding site referred to as the metal ion dependent adhesion site (MIDAS). Upon binding, the Mg^{2+} ion of the MIDAS coordinates an acidic side chain of the ligand [2] (and references therein).

On resting cells, integrins are predominantly found in a "bent" configuration, and bind ligand only weakly. Upon activation by intracellular or extracellular signals, integrins "extend" and bind ligand with high affinity [3,4]. Integrin ligands include cell surface proteins, components of the extracellular matrix, sulfated glycosaminoglycans, and plasma proteins such as fibrinogen and complement [5]. Important ligands for the family of β2 integrins are the intercellular adhesion molecules (ICAMs). These are homologous cell surface proteins with immunoglobulin superfamily domains. The integrin αLβ2 binds strongly to ICAM-1. Integrin αLβ2 is expressed on leukocytes and ICAM-1 is upregulated on many cell types by inflammatory cytokines, facilitating adhesion to

* Corresponding author. Tel.: +1 617 278 3200; fax: +1 617 278 3232.
E-mail address: springeroffice@cbr.med.harvard.edu (T.A. Springer).
[1] These authors contributed equally to this work.

1570-9639/$ - see front matter © 2007 Elsevier B.V. All rights reserved.
doi:10.1016/j.bbapap.2007.06.014

leukocytes in immune responses. Detailed analyses have shown how the global changes in the conformation of αLβ2 are propagated to the I domain [6–8]. High-affinity ligand binding by integrin I domains requires a conformation of the domain referred to as "open", while the "closed" conformation has an affinity for ligand that is several orders of magnitude lower [2].

While the importance of conformational changes within isolated I domains in regulating ligand binding has been reported [9–13], the relationship between metal ion binding affinity and ligand binding affinity by the I domains has not been elucidated. Past studies of the binding of I domains to their natural ligands measured the affinity of the interaction by application of a single Mg^{2+} concentration, e.g., at 1 mM, which approximates the Mg^{2+} concentration in human plasma under physiological conditions [9–12].

Here we use αL I domains that are wild-type or have engineered disulfide bonds or point mutations that stabilize the I domain into conformations that exhibit either an intermediate or high affinity for ligand. Isothermal titration calorimetry (ITC) and surface plasmon resonance (SPR) are used to extend earlier binding studies on integrin I domains by using a range of metal concentrations. Further, it is known that Mn^{2+} can substitute for Mg^{2+} at the MIDAS [14] and support binding of the αL I domain to ICAM-1 [15]. Therefore, Mn^{2+} was included in ITC titrations to determine the generality of the trends seen with Mg^{2+}.

The results suggest an inverse relationship between the affinity of the I domain for metal ions and the affinity for ligand. Conformations of the αL I domain that exhibit a high affinity for the ligand ICAM-1 have a low affinity for metal. This trend is discussed in the context of structural data and modeling studies to provide a better understanding of the function and regulation of integrins containing I domains.

2. Materials and methods

2.1. Recombinant I domains

The wild-type (Wt) αL I domain and two constructs with introduced disulfide bonds that support ICAM-1 binding with high affinity (the E284C/E301C mutant) or intermediate affinity (the L161C/F299C mutant) [16], and the intermediate affinity F292A mutant [17] were recovered from *E. coli* inclusion bodies and refolded as described [9]. All proteins were mixed with 50 mM EDTA before a final purification step by gel permeation chromatography in buffer containing 150 mM NaCl, 20 mM Tris–HCl, pH 7.4. The protein concentration was estimated from the optical absorption of the protein sample. From the primary structure of the wild-type domain (G-128 to Y-307) the extinction coefficient was calculated to be 8940 $M^{-1}\cdot cm^{-1}$ corresponding to an A280 of 0.44 at a protein concentration of 1 mg/ml. The mutations only marginally changed the predicted extinction coefficient. For all constructs estimates of the protein concentrations based on the optical absorbance were in good agreement with values obtained from a Bradford assay (Pierce, Rockford, IL).

2.2. Isothermal calorimetry

ITC was carried out essentially as described by Baldwin *et al.* [18]. Protein samples were loaded into a microcalorimeter (VP-ITC, MicroCal, Northampton, MA) with a cell volume of 1.4512 ml (V_c). The αL I domains were loaded in 150 mM NaCl, 20 mM Tris–HCl, pH 7.4, at concentrations of 63 μM (Wt, L161C/F299C, and E284C/E301C constructs) or 32 μM (F292A). Titrations with metal ions at 3.5 mM in matching buffer were monitored for 50 injections of 2 or 3 μl (V_{inj}) with continuous stirring at 200 rpm. The recorded heats for each injection (q_i) were fit to the equation:

$$q_i = \langle H\rangle_i \cdot V_c \cdot n \cdot M_i - \langle H\rangle_{i-1} \cdot (V_c - V_{inj}) \cdot n \cdot M_{i-1} + b \quad (1)$$

where M_i is the total I domain concentration, n is the stoichiometry of interaction, and b is a constant baseline term to account for dilution heats and viscous mixing. $\langle H\rangle$ is the excess enthalpy defined in Eq. (2) for a 1:1 binding model:

$$\langle H\rangle = \frac{K_A \cdot x}{1 + K_A \cdot x} \cdot \Delta H^0 \quad (2)$$

where K_A is the association constant for metal binding by the I domain, x is the concentration of free metal, and ΔH^0 the enthalpy of the reaction. The entropy, ΔS^0, was calculated from the relation:

$$\Delta G^0 = -R \cdot T \cdot \ln K_A = \Delta H^0 - T \cdot \Delta S^0 \quad (3)$$

where R is the gas constant at 8.315 $J\cdot K^{-1}\cdot mol^{-1}$ and T is the temperature set at 299 K (26 °C) in all experiments. Non-linear least square fitting of Eq. (1) to the experimental data was accomplished as described [19].

The stoichiometries reported here deviate from the expected 1:1 ratio. We note that multiple protein preparations were used to obtain enough material for all of the titrations. There is considerable variability in the refolding and purification process, likely contributing significant errors in determining the active protein concentration. If the error is due solely to determining the active protein concentration, then the stoichiometry will simply be a correction factor and will not affect the fitted parameters. Previous reports using ITC with integrin I domains did not report stoichiometries [18,20].

2.3. Surface plasmon resonance assays

SPR measurements were carried out essentially as described earlier with modifications to accommodate varying levels of Mg^{2+} [9]. The binding of αL I domains was measured in CM-5 chip (Biacore, Uppsala, Sweden) flow cells with either 2500 response units (RU; 1000 RU ~ 1 ng protein per mm^2 of flow cell surface) or 3500 RU of amine-coupled ICAM-1. As reference, a flow cell activated as for the coupling of ligand and blocked with ethanolamine was employed in series with the ligand-coupled flow cell. Samples of the αL I domain were diluted in running buffer containing 150 mM NaCl, 20 mM Tris–HCl, pH 7.4 (TBS) with $MgCl_2$ added in concentrations from 0.1 mM to 10 mM for the intermediate and high affinity I domains or 0.5 mM to 10 mM for the wild-type I domain. For all experiments the flow rate was at 10 μl/min with data collection at 5 Hz.

SPR data analysis was carried out by recording the steady state equilibrium response level as a function of the injected protein and Mg^{2+} concentrations. A two-step reaction scheme was employed to describe the influence of the concentration of Mg^{2+} on the I domain ligand binding:

$$I + Mg^{2+} \leftrightarrow I\bullet Mg^{2+} \overset{L}{\leftrightarrow} I\bullet Mg^{2+}\bullet L \quad (4)$$

where I is the I domain and L is the ligand ICAM-1 coupled to the flow cell surface. The observed binding event is that of the metal-loaded I domain to the surface-coupled ligand. For a binding event following Langmuir adsorption isotherms, Eq. (5) applies:

$$R_{eq} = R_{max} \cdot K_{I\bullet Mg} \cdot \frac{c_{I\bullet Mg}}{1 + K_{I\bullet Mg} \cdot c_{I\bullet Mg}} \quad (5)$$

where R_{eq} is the observed equilibrium response, R_{max} is the maximum response obtainable for complete saturation of ligand binding sites on the surface, $K_{I\bullet Mg}$ is the association constant for metal-loaded I domain binding to the immobilized ligand, and $c_{I\bullet Mg}$ is the free concentration of metal-loaded I domain. For the scheme presented in Eq. (4), the equilibrium between the metal ion and I domain in the flow stream is used to determine the concentration of metal-loaded I domain:

$$c_{I\bullet Mg} = K_{Mg} \cdot c_{Mg} \cdot c_I \quad (6)$$

where K_{Mg} is the affinity of metal ion for the I domain, and c_{Mg} and c_I are the free concentrations of metal and I domain, respectively. The flow stream concentration of I domain not in complex with metal is calculated from the known total I domain ($c_{I,tot}$) concentration as:

$$c_{I,tot} = c_I + c_{I\bullet Mg} \quad (7)$$

By substituting Eq. (6) and rearranging, the free I domain concentration was defined as:

$$c_I = \frac{c_{I,tot}}{1 + K_{Mg} \cdot c_{Mg}} \quad (8)$$

This approximation is valid since any I domain that is removed from the flow stream and bound to the surface ligand is replenished by the incoming equilibrated solution of metal and I domain, keeping the free I domain concentration constant. The free metal concentration is set to be equal to the total metal concentration since the total concentration far exceeded the total I domain concentration in all experiments.

Eq. (9), obtained by substituting Eqs. (6) and (8) into (5), was used to globally fit a data set containing all of the observed equilibrium responses for the range of metal and protein concentrations for a given I domain:

$$R_{eq} = \frac{R_{max} \cdot K_{Mg} \cdot K_{I\bullet Mg} \cdot \left(\frac{c_{I,tot}}{1+K_{Mg} \cdot c_{Mg}}\right) \cdot c_{Mg}}{1 + K_{Mg} \cdot K_{I\bullet Mg} \cdot \left(\frac{c_{I,tot}}{1+K_{Mg} \cdot c_{Mg}}\right) \cdot c_{Mg}} + b_i \quad (9)$$

where b_i is a baseline term, one for each metal concentration, that corrects for a small off-set in the response level generated by the difference in metal-containing buffer flowing over the reference surface versus the protein-coupled surface.

3. Results

3.1. ITC measurements of the divalent metal cation affinities to wild-type and mutant αL I domains

The raw ITC data for titrations of various metals into wild-type αL I domain are shown in Fig. 1. Fits of the data to Eq. (1) are indicated by solid lines in Fig. 1 with determined values given in Fig. 2A. The metal affinities are highest for Mn^{2+} at 3.16 μM (3.16×10^5 M^{-1}), second highest for Mg^{2+} at 19.42 μM (5.15×10^4 M^{-1}), and weakest for Ca^{2+} at 384 μM (2600 M^{-1}). The affinities are weak yet in a reasonable range for measurement by ITC [21], and the reaction is continued to near complete saturation of the metal binding site, giving more confidence in the determination of the association constants, although determinations of the enthalpy are less reliable [22]. The trend in metal affinities obtained for the αL I domain is

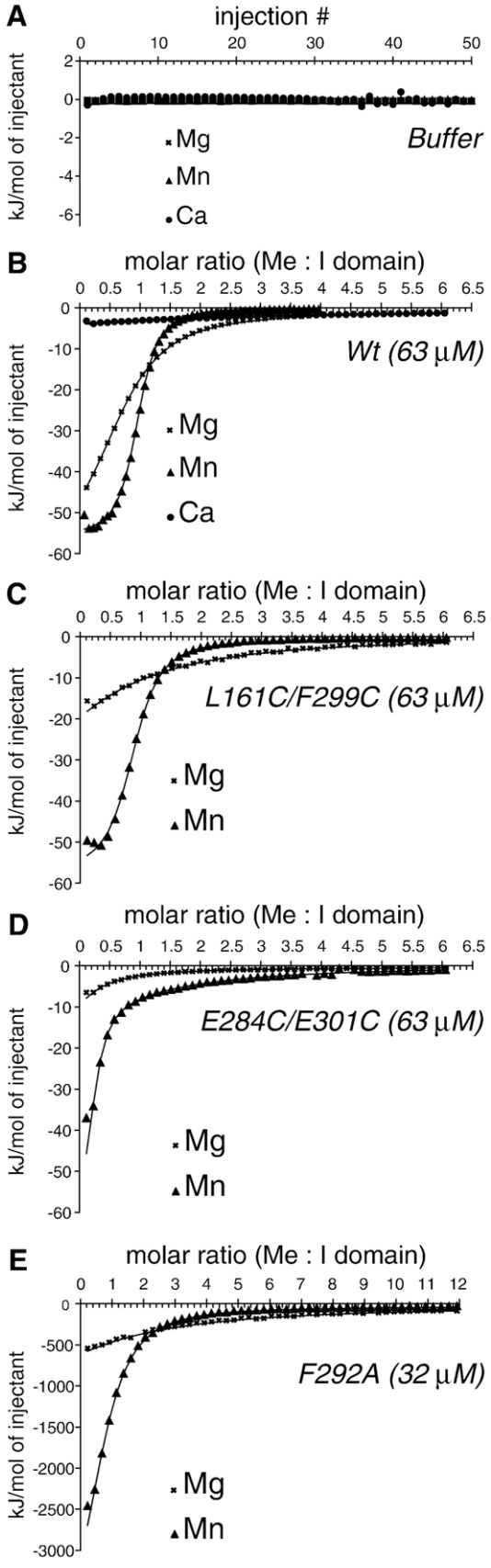

Fig. 1. Isothermal calorimetry measurements of the interaction between divalent metal ions and αL I domain constructs. (A) Control experiment with the heat development (in kJ normalized to mol of injected metal ion) for the series of 50 injections (V_{inj}=3 μl) of either 3.5 mM $MgCl_2$, $MnCl_2$, or $CaCl_2$ contained in TBS into TBS without added divalent cations. In Panel B–E, the heat development (in kJ normalized to mol of injected metal ion) is shown as a function of the molar ratio of metal ion (Me) to I domain. Solid lines show the best least square fit according to Eq. (1) of the integrated heat developments for the wild-type and L161C/F299C constructs or according to Eq. (10) for the E284C/E301C construct. (B) Injection of $MgCl_2$, $MnCl_2$, and $CaCl_2$ into 63 μM of wild-type construct. V_{inj} was at 3 μl for $MgCl_2$ and $CaCl_2$ injections and at 2 μl for $MnCl_2$ injections. (C) Injection of $MgCl_2$ or $MnCl_2$ (V_{inj}=3 μl) into 63 μM L161C/F299C construct. (D) Injection of $MgCl_2$ or $MnCl_2$ (V_{inj}=3 μl) into 63 μM E284C/E301C construct. (E) Injection of $MgCl_2$ or $MnCl_2$ (V_{inj}=3 μl) into 32 μM F292A construct.

A

$$I + Me^{2+} \underset{}{\overset{K_{Me}}{\rightleftharpoons}} I{\cdot}Me^{2+}$$

I domain	Me^{2+}	K_{Me} $M^{-1}/10^3$	ΔH^0 kJ·mol^{-1}	ΔS^0 J·K^{-1}·mol^{-1}	n
Wt	Mg^{2+}	51.5±0.9	-63.1±0.2	-121.1±0.5	0.71±0.01
	Mn^{2+}	316±6	-37.40±0.03	-19.8±0.16	1.34±0.002
L161C/F299C	Mg^{2+}	8.4±0.3	-80.3±1.8	-193±6	0.58±0.05
	Mn^{2+}	229±10	-58.5±0.1	-93.7±0.6	0.86±0.04
E284C/E301C	Mg^{2+} *species I*	1.01±0.14	-33.7±0.7	-12.0±2.7	1 {(0.82±0.02)
	species II	29.0±1.3	-20.8±0.7	-27.2±2.4	(0.18±0.02)}
	Mn^{2+} *species I*	8.4±0.9	-28.5±9.9	-20.3±1.7	1 {(0.78±0.01)
	species II	254±36	-29.8±0.4	-894±30	(0.22±0.01)}
F292A	Mg^{2+}	6.6±0.2	-3,024±53	-10,020±176	1.03±0.07
	Mn^{2+}	70.8±1.9	-4,419±29	-14,685±97	0.72±0.02

B

$$I + Mg^{2+} \underset{}{\overset{K_{Mg}}{\rightleftharpoons}} I{\cdot}Mg^{2+} \underset{L}{\overset{K_{I{\cdot}Mg}}{\rightleftharpoons}} I{\cdot}Mg^{2+}{\cdot}L$$

I domain	K_{Mg} ($M^{-1}/10^3$)	$K_{I{\cdot}Mg}$ ($M^{-1}/10^4$)
Wt	1.23±0.12	1.6±1.4
L161C/F299C	3.37±0.60	152±50
E284C/E301C	0.46±0.14	898±111
F292A	2.28±0.44	12.2±1.3

Fig. 2. (A) Binding constants reported as dissociation constants (K_{Me} in μM), enthalpies (ΔH^0 in kJ·mol^{-1}), entropies (ΔS^0 in J·K^{-1}·mol^{-1}), and stoichiometries (n) for the divalent metal ion binding by the wild-type, F292A and L161C/F299C αL I domain constructs estimated by isothermal calorimetry according to Eq. (1). As described in text, the heat development for the E284C/E301C αL I domain construct was fitted to Eq. (10) with two species of non-equilibrating metal-binding species. For each species the estimated association constant and thermodynamic parameters are listed based on the assumption that the total I domain concentration equals the total concentration of binding sites with the fraction of species I and species II binding sites listed in brackets. The standard error and propagated error for the calculation of ΔS^0 through Eq. (3) was calculated as described [29]. (B) Association constants for Mg^{2+} binding (K_{Mg}) by the αL domains and association constants ($K_{Mg\bullet I}$) for Mg^{2+}-loaded αL domain binding to ICAM-1 estimated according to Eq. (9) from SPR measurements.

consistent with the trends of metal binding to the wild-type αM I domain reported by others [18,20].

To assess metal binding to conformations of the I domain resembling the ligand bound form (open conformation), we employed two αL I domain constructs [9,16] that contain disulphide bonds designed to favor the open conformation over the closed conformation. Previous measurements in 1 mM Mg^{2+} show that the wild-type I domain has low affinity for ICAM-1 ($K_d \sim 1500$ μM). Under the same conditions, the L161C/F299C construct has an intermediate affinity for ICAM-1 ($K_d \sim 3$ μM). This construct bound Mg^{2+} ions at approximately 120 μM (8000 M^{-1}), or 6-fold lower than wild-type αL I domain. The affinity of the L161C/F299C construct for the stronger binding Mn^{2+}-ion at ~4 μM (229,000 M^{-1}) was only slightly lower than the affinity of Mn^{2+} for the wild-type domain (Figs. 1C and 2A). Interestingly, this intermediate affinity construct, when not bound to ICAM-1, shows a conformation of the MIDAS that is similar to the wild-type MIDAS [16]. However, the loop connecting strand β6 and helix α7 adopts a conformation that is intermediate between the closed and open structures and is thought to predispose the MIDAS for a conformational change to the open conformation, as is seen when this mutant binds to ICAM-1 [16] (Fig. 3).

The E284C/E301C construct displays a high affinity ($K_d \sim 0.36$ μM) for ICAM-1 at 1 mM Mg^{2+} [9,16]. The crystal structure of another I domain construct with high affinity for ICAM-1 that is also stabilized by an introduced disulfide in roughly the same region is shown in Fig. 3; no structure is available for the E284C/E301C construct used here. In the high affinity open conformation there is a more drastic shift in the

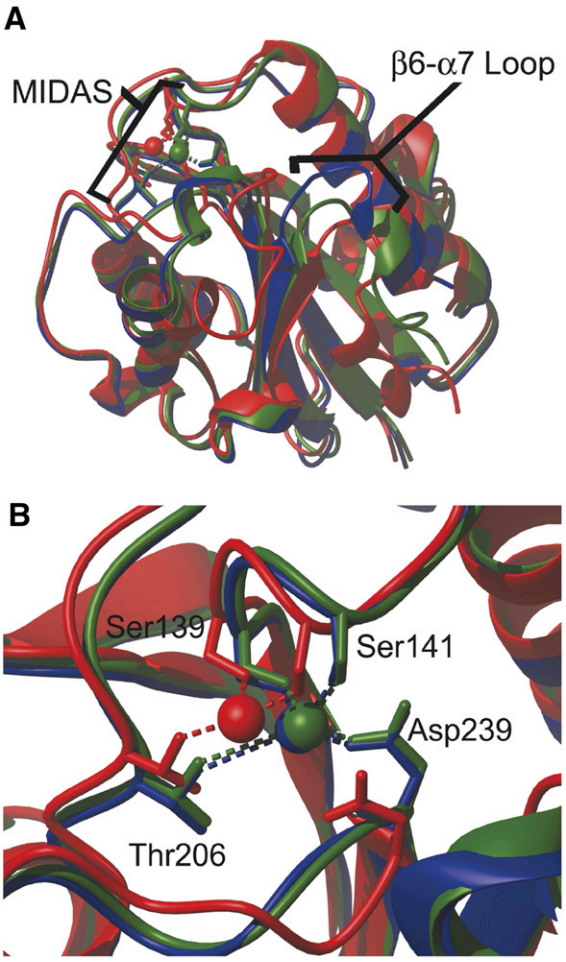

Fig. 3. (A) Overlay of the crystal structures of wild-type αL I domain (PDB ID 1ZOP) in black, the intermediate affinity I domain (PDB ID 1MJN) in grey, and a disulfide bonded high affinity αL I domain (PDB ID 1MQ9, not the high-affinity construct used in this study) in white. The differences in the β6-α7 loop are highlighted. (B) Close-up view of metal coordination at the MIDAS in each of the constructs. Metal ions are shown as spheres. Residues that directly coordinate the metal ions are shown as sticks, with dashed lines representing metal coordinations.

β6-α7 loop than in the intermediate conformation (Fig. 3A). Furthermore, the MIDAS is in the open conformation. The loop containing Asp239 no longer directly coordinates the metal ion at the MIDAS, and instead, Thr206 provides a contact to the metal ion (Fig. 3B). However, when titrated with metal ions (Fig. 1D), fitting the titrations to Eq. (1) resulted in unreasonably low stoichiometry, i.e., $n \ll 1$ (data not shown). Colorimetric quantification of the free sulhydryl groups by incubation with 5,5′-dithio-*bis*-(2-nitrobenzoic acid) (Pierce) showed that approximately 20% of the I domains had not formed the disulfide bond and hence would be expected to assume a conformation similar to the wild-type construct. For this construct, the heat development for the injections was formulated as a sum of binding reactions involving two non-equilibrating I domain species, here termed species I and species II. The concentrations of the two species are given as $f{\cdot}M_i$ and $(1-f){\cdot}M_i$ with M_i as the total I domain concentration and f as the fraction of species I binding sites in the sample. Eq. (1) was consequently modified to:

$$\begin{aligned} q_i = {} & \langle H\rangle_{I,i}\cdot V_c\cdot f\cdot M_i - \langle H\rangle_{I,i-1}\cdot(V_c - V_{inj})\cdot f\cdot M_{i-1} \\ & + \langle H\rangle_{II,i}\cdot V_c\cdot(1-f)\cdot M_i - \langle H\rangle_{II,i-1}\cdot(V_c - V_{inj}) \\ & \cdot(1-f)\cdot M_{i-1} + b \end{aligned} \tag{10}$$

where the excess enthalpies are related to ΔH_I^0 and ΔH_{II}^0 and the association constants for each species of binding sites ($K_{A,I}$ and $K_{A,II}$) are described by Eq. (2). As shown in Fig. 2A, fitting of Eq. (10) to the heats developed from the open conformation construct (Fig. 1D) assigned one population of 80% of the I domain binding sites with an affinity for Mg^{2+} ($K_d \sim 990$ μM) 50-fold lower than the wild-type construct ($K_d \sim 19$ μM) (species I). The remaining 20% of the I domains (species II) bound Mg^{2+} with an affinity ($K_d \sim 34$ μM) comparable to the wild-type, in agreement with the finding that 20% of the I domains lacked a disulfide bond and would be expected to bind metal similarly to wild-type.

Molecular dynamics [23] and mutational evidence from the αM I domain [13] and αL I domain [17] supports a crucial role for Phe-292 in stabilizing the αL I domain in the closed conformation. The F292A mutant αL I domain has intermediate affinity for ICAM-1 [17]. The affinity of the F292A mutant αL I domain for Mg^{2+} and Mn^{2+} measured by ITC (Fig. 1E) and fitted to Eq. (1) was 8-fold and 4.5-fold lower, respectively, than the affinity of the wild-type construct (Fig. 2A).

Constructs known to resemble the ligand bound conformation in some structural features result in lower metal binding affinities than wild-type as determined by ITC. Fig. 2A also reports the determined enthalpies and entropies for each construct. We observe that Mg^{2+} tends to be more enthalpically favored than Mn^{2+} binding for each construct. Beyond this, no clear correlations or explanations for the observations are apparent.

3.2. Influence of the metal ion concentration on the binding of αL I domains to ICAM-1

Surface plasmon resonance was used to monitor the binding of each αL I domain to the protein ligand ICAM-1. The binding of ICAMs by αL I domain constructs is dependent on Mg^{2+} or Mn^{2+} as shown by ligand binding assays and crystal structures [9,16,24]. Absolutely no binding is detected in the presence of EDTA. Based on these observations the observed equilibrium response in the SPR assay is described by Eq. (9). The model indicates that only a metal bound I domain can form a complex with the ICAM-1 on the chip surface (Eq. (4)). This model does not attempt to explicitly incorporate any equilibrium in the wild-type I domain between closed and open conformations, since such a model leads to highly correlated parameters, and hence unreliable data fits. This is addressed more completely in the discussion. Equilibration between open and closed conformations is not expected for the disulphide bonded constructs.

Fig. 4 shows representative response curves generated for each of the constructs binding to immobilized ICAM-1 as a function of varying Mg^{2+} concentration. The curves in each panel are

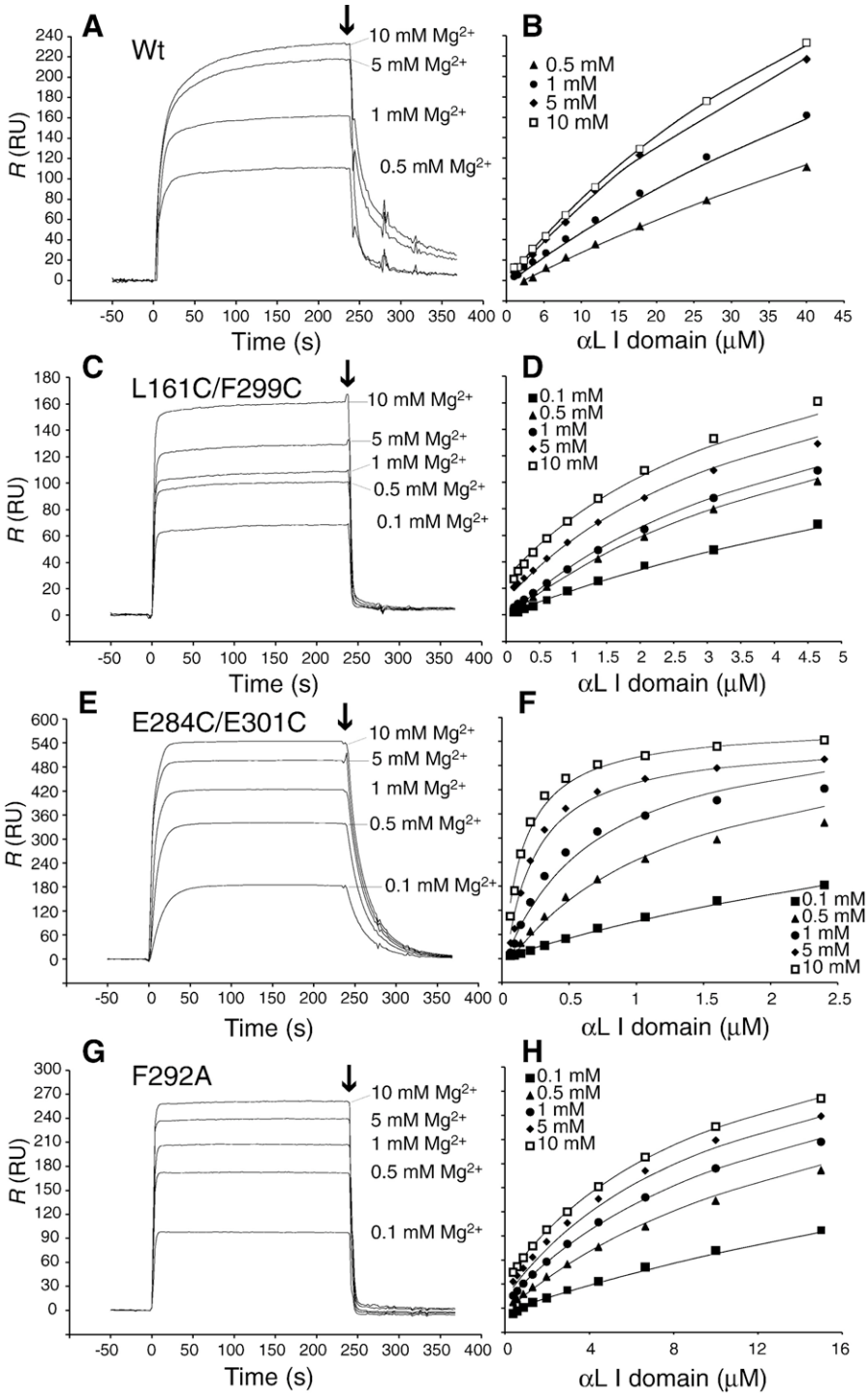

Fig. 4. SPR measurements on the influence of Mg^{2+} concentration on ICAM-1 binding by the αL I domain constructs. Binding was measured for the wild-type (A, B), the L161C/F299C (C, D), E284C/E301C (E, F), and F292A-mutated (G, H) constructs. For comparison the sensorgrams are shown for injection of the αL wild-type, L161C/F299C, and E284C/E301C constructs in the presence of Mg^{2+} at concentrations between 0.1 mM and 10 mM with the maximal applied I domain concentration at 40 μM for the wild-type construct (panel A), at 4.6 μM for the L161C/F299C construct (panel C), at 2.4 μM for the E284C/E301C construct (panel E), and at 15 μM for the F292A-mutated construct (panel G). The ends of the injection phases are indicated with arrows. In panels B, D, F, H representative equilibrium responses (R_{eq}) are shown for each construct (wild-type, L161C/F299C, E284C/E301C, and F292A, respectively) at all tested I domain and Mg^{2+} concentrations. Solid lines indicate the calculated R_{eq} based on the estimated K_{Mg} and $K_{Mg\bullet I}$ according to Eq. (9).

generated at a given I domain concentration. Also shown are the steady state response levels plotted as a function of I domain concentration. From the response levels observed at varying I domain and Mg^{2+} concentrations, affinity estimates from fits to Eq. (9) are shown in Fig. 2B. This simple model adequately captures all of the data for each construct.

The affinities of the metal-loaded αL I domains for ICAM-1 ($K_{I\bullet Mg}$) are in excellent agreement with previous findings in

1 mM Mg^{2+} for the intermediate affinity (L161C/F299C), and high affinity (E284C/E301C) mutants (Fig. 2B) [9,16,17]. The affinity of Mg^{2+} for the disulphide constrained constructs estimated from SPR was similar to that estimated by ITC within a factor of two. Considering the use of different methods (ITC being direct and SPR being an indirect measure of metal affinity), and the variability in protein preparations, we consider affinities within a factor of two to three to be similar. In contrast, the observed affinity for Mg^{2+} of the wild-type αL I domain estimated by SPR was about 40-fold lower than that estimated by ITC. This is a significant difference and is discussed in detail below.

4. Discussion

Here, by ITC we show that the wild-type αL I domain has an affinity for metals in the order of $Mn^{2+} > Mg^{2+} > Ca^{2+}$. This is consistent with theoretical work that considers the coordination preferences of these ions in the context of the αL I domain [25], and experimental work reported by others on the αM I domain [18,20]. This trend also holds for the constructs displaying higher affinity for ligand.

In this study we report the ΔH^0 and ΔS^0 for the binding of Mn^{2+} and Mg^{2+} to the αL I domain. Although we found a systematic lowering of metal ion affinity with stabilization of the open conformation of the I domain we were not able to assign this change to alteration in either ΔH^0 or ΔS^0 but must assign these affinity differences between the constructs to concurrent alterations in both thermodynamic variables. However, a striking finding in this study was the pronounced difference between the wild-type, L161C/F299C, and E284C/E301C constructs versus the F292A construct with regard to the magnitude of ΔH^0 and ΔS^0. We suggest that this difference reflects rearrangements in the protein structure of F292A upon the binding of metal ions. This seems consistent with the structural rationale for how this mutation favors the open conformation of the domain by loosening the interaction between the β6-α7 loop and the body of the domain. This may make the structure more labile in comparison with the wild-type and disulphide-stabilized constructs. Nevertheless, the F292A construct fits into the pattern of an inverse relationship between metal ion affinity and ligand affinity. The ITC data also indicate that I domain constructs displaying an affinity for protein ligand that is higher than wild-type have a lower affinity for metal ions. Fig. 3A depicts an overlay of three crystal structures of the αL I domain. When bound to a ligand, the metal ion at the MIDAS is contacted by an acidic side chain of the ligand [1,2,14,26]. Prior to ligand binding, in the closed conformation (low affinity for ligand), the metal ion is liganded by three MIDAS residues, Ser139, Ser141, and Asp239, through direct (inner sphere) coordinations. In the open conformation (high affinity for ligand), direct coordination with the aspartate residue is replaced by a threonine hydroxyl group (see Fig. 3B), although the aspartate maintains an indirect (outer sphere) coordination to the metal ion through an intervening water molecule [14].

This alteration in metal ion coordination is predicted to have several effects. It increases the electrophilicity of the metal ion, promoting direct coordination by an acidic residue of the ligand [14,16,26]. Further, for a Mg^{2+} ion chelated by non-aqueous ligands, the replacement of one charged ligand with a polar ligand (Asp239 for Thr206 in Fig. 3B) in the primary coordination sphere greatly enhances the subsequent binding of a negatively charged group from the ligand [27]. This agrees with the earlier suggestion [14] that the conformational change in the open MIDAS enhances its electrophilicity and promotes ligand binding.

Ajroud et al. [20] reported from ITC measurements that the observed affinity for Mg^{2+} of an αM I domain mutated in the C-terminal helix α7 helix to favor the open conformation [10] increased 9 fold in comparison with the wild-type domain. However, the open-conformation αM I domain binds promiscuously to protein species through a strong affinity for glutamate side chains [12]. At the high protein concentrations used for ITC, a thermal contribution from homotypic interactions between αM I domains as seen in crystal lattice contacts[14] is thus difficult to rule out. By contrast, the open-conformation αL I domain has a markedly lower affinity for glutamate than the αM I domain [12] and is thus a better model for studying the metal ion-binding by open-conformation I domains in the absence of homotypic interactions confounding the ITC measurements.

Additional rearrangements in the loops that bear MIDAS residues increase the surface complementarity of the I domain surface for ligand. Magnetic resonance studies on the wild-type αL I domain [28] showed that high concentrations of ligand altered the chemical shifts of residues known from crystal structures to be involved in shape shifting from the closed toward the open conformation. These observations support the idea that only the open conformation of the I domain MIDAS is competent for ligand binding. This is how we have interpreted the SPR data.

Based on the above observations, the SPR data presented here was fit to a model that considers the observed response to be due to the binding of an open conformation I domain that is already coordinating a metal ion. For the intermediate and high affinity constructs, the Mg^{2+} affinities determined by SPR are consistent with those measured by ITC. For the wild-type I domain, the Mg^{2+} affinities determined by ITC are 40-fold higher than those determined by SPR. The difference is that the wild-type construct is in equilibrium between closed and open conformations, and is predominantly in the closed conformation with low affinity for ligand, whereas the mutant constructs are stabilized in conformations with higher affinity for ligand. As such, the model in Eq. (4) captures the metal-I domain-ICAM-1 equilibria appropriately. However, in the case of the wild-type construct an additional equilibrium underlies the observed binding of metal-loaded open conformation I domain to ICAM-1, i.e. the equilibrium between the open and closed I domain conformations. A large number of previous studies show that the wild-type I domain heavily favors a closed conformation. With the underlying conformational equilibrium pulling towards a closed I domain, the binding competent concentration is lower than estimated if no conformational equilibrium is present. Thus, the SPR estimates of the Mg^{2+} affinity reflect binding to the small population of open ligand binding-competent conformation, while the Mg^{2+} binding results with the wild-type I domain by ITC reflect binding to the predominant population of closed conformation. This model is

consistent with the need for integrins to be activated by intracellular or extracellular signals for binding competency.

The lower affinity for Mg^{2+} of the open compared to the closed conformation of the αL I domain suggests a mechanism whereby the Mg^{2+} ion of the I domain MIDAS has higher propensity for coordination to the side chain of a ligand glutamate at the cost of lower I domain affinity for the metal ion. However, since physiologic plasma Mg^{2+} concentration is in the range of 0.7 to 1.05 mM, i.e. near the K_d of Mg^{2+} for the open I domain, the lower affinity for Mg^{2+} has little effect on overall binding to ICAM-1.

Acknowledgements

We thank Drs. Joonil Seog and Romualdas Stapulionis for their critical reading of the manuscript. Supported by NIH grant CA31798.

References

[1] J.-O. Lee, P. Rieu, M.A. Arnaout, R. Liddington, Crystal structure of the A domain from the a subunit of integrin CR3 (CD11b/CD18), Cell 80 (1995) 631–638.
[2] M. Shimaoka, J. Takagi, T.A. Springer, Conformational regulation of integrin structure and function, Annu. Rev. Biophys. Biomol. Struct. 31 (2002) 485–516.
[3] B.-H. Luo, J. Takagi, T.A. Springer, Locking the β3 integrin I-like domain into high and low affinity conformations with disulfides, J. Biol. Chem. 279 (2004) 10215–10221.
[4] J. Takagi, T.A. Springer, Integrin activation and structural rearrangement, Immunol. Rev. 186 (2002) 141–163.
[5] T.A. Springer, Adhesion receptors of the immune system, Nature 346 (1990) 425–433.
[6] W. Yang, M. Shimaoka, J.F. Chen, T.A. Springer, Activation of integrin β subunit I-like domains by one-turn C-terminal a-helix deletions, Proc. Natl. Acad. Sci. U. S. A. 101 (2004) 2333–2338.
[7] W. Yang, M. Shimaoka, A. Salas, J. Takagi, T.A. Springer, Inter-subunit signal transmission in integrins by a receptor-like interaction with a pull spring, Proc. Natl. Acad. Sci. U. S. A. 101 (2004) 2906–2911.
[8] N. Nishida, C. Xie, M. Shimaoka, Y. Cheng, T. Walz, T.A. Springer, Activation of leukocyte β2 integrins by conversion from bent to extended conformations, Immunity 25 (2006) 583–594.
[9] M. Shimaoka, C. Lu, R. Palframan, U.H. von Andrian, J. Takagi, T.A. Springer, Reversibly locking a protein fold in an active conformation with a disulfide bond: integrin αL I domains with high affinity and antagonist activity in vivo, Proc. Natl. Acad. Sci. U. S. A. 98 (2001) 6009–6014.
[10] J.-P. Xiong, R. Li, M. Essafi, T. Stehle, M.A. Arnaout, An isoleucine-based allosteric switch controls affinity and shape shifting in integrin CD11b A-domain, J. Biol. Chem. 275 (2000) 38762–38767.
[11] T. Vorup-Jensen, C. Ostermeier, M. Shimaoka, U. Hommel, T.A. Springer, Structure and allosteric regulation of the αXβ2 integrin I domain, Proc. Natl. Acad. Sci. U. S. A. 100 (2003) 1873–1878.
[12] T. Vorup-Jensen, C.V. Carman, M. Shimaoka, P. Schuck, J. Svitel, T.A. Springer, Exposure of acidic residues as a danger signal for recognition of fibrinogen and other macromolecules by integrin αXβ2, Proc. Natl. Acad. Sci. U. S. A. 102 (2005) 1614–1619.
[13] R. Li, P. Rieu, D.L. Griffith, D. Scott, M.A. Arnaout, Two functional states of the CD11b A-domain: correlations with key features of two Mn^{2+}-complexed crystal structures, J. Cell Biol. 143 (1998) 1523–1534.
[14] J.-O. Lee, L.A. Bankston, M.A. Arnaout, R.C. Liddington, Two conformations of the integrin A-domain (I-domain): a pathway for activation? Structure 3 (1995) 1333–1340.
[15] M. Shimaoka, A. Salas, W. Yang, G. Weitz-Schmidt, T.A. Springer, Small molecule integrin antagonists that bind to the β2 subunit I-like domain and activate signals in one direction and block them in another, Immunity 19 (2003) 391–402.
[16] M. Shimaoka, T. Xiao, J.-H. Liu, Y. Yang, Y. Dong, C.-D. Jun, A. McCormack, R. Zhang, A. Joachimiak, J. Takagi, J.-H. Wang, T.A. Springer, Structures of the αL I domain and its complex with ICAM-1 reveal a shape-shifting pathway for integrin regulation, Cell 112 (2003) 99–111.
[17] M. Jin, G. Song, Y.-S. Kim, N. Astrof, M. Shimaoka, D. Wittrup, T.A. Springer, Directed evolution to probe protein allostery and integrin I domains of 200,000-fold higher affinity, Proc. Natl. Acad. U. S. A. 103 (2006) 5758–5763.
[18] E.T. Baldwin, R.W. Sarver, G.L. Bryant Jr., K.A. Curry, M.B. Fairbanks, B.C. Finzel, R.L. Garlick, R.L. Heinrikson, N.C. Horton, L.L. Kelley, A.M. Mildner, J.B. Moon, J.E. Mott, V.T. Mutchler, C.S. Tomich, K.D. Watenpaugh, V.H. Wiley, Cation binding to the integrin CD11b I domain and activation model assessment, Structure 6 (1998) 923–935.
[19] T.T. Waldron, M.A. Modestou, K.P. Murphy, Anion binding to a protein–protein complex lacks dependence on net charge, Protein Sci. 12 (2003) 871–874.
[20] K. Ajroud, T. Sugimori, W.H. Goldmann, D.M. Fathallah, J.P. Xiong, M.A. Arnaout, Binding affinity of metal ions to the CD11b A-domain is regulated by integrin activation and ligands, J. Biol. Chem. 279 (2004) 25483–25488.
[21] W.B. Turnbull, A.H. Daranas, On the value of c: can low affinity systems be studied by isothermal titration calorimetry? J. Am. Chem. Soc. 125 (2003) 14859–14866.
[22] J. Tellinghuisen, Optimizing experimental parameters in isothermal titration calorimetry, J. Phys. Chem., B Condens. Matter Mater. Surf. Interfaces Biophys. 109 (2005) 20027–20035.
[23] M. Jin, I. Andricioaei, T.A. Springer, Conversion between three conformational states of integrin I domains with a C-terminal pull spring studied with molecular dynamics, Structure 12 (2004) 2137–2147.
[24] G. Song, Y. Yang, J.-H. Liu, J. Casasnovas, M. Shimaoka, T.A. Springer, J.-H. Wang, An atomic resolution view of ICAM recognition in a complex between the binding domains of ICAM-3 and integrin αLβ2, Proc. Natl. Acad. Sci. U. S. A. 102 (2005) 3366–3371.
[25] E. San Sebastian, J.M. Mercero, R.H. Stote, A. Dejaegere, F.P. Cossio, X. Lopez, On the affinity regulation of the metal-ion-dependent adhesion sites in integrins, J. Am. Chem. Soc. 128 (2006) 3554–3563.
[26] J. Emsley, C.G. Knight, R.W. Farndale, M.J. Barnes, R.C. Liddington, Structural basis of collagen recognition by integrin α2β1, Cell 101 (2000) 47–56.
[27] T. Dudev, C. Lim, Principles governing Mg, Ca, and Zn binding and selectivity in proteins, Chem. Rev. 103 (2003) 773–788.
[28] J.R. Huth, E.T. Olejniczak, R. Mendoza, H. Liang, E.A. Harris, M.L. Lupher Jr., A.E. Wilson, S.W. Fesik, D.E. Staunton, NMR and mutagenesis evidence for an I domain allosteric site that regulates lymphocyte function-associated antigen 1 ligand binding, Proc. Natl. Acad. Sci. U. S. A. 97 (2000) 5231–5236.
[29] P.R. Bevington, D.K. Robinson, Data reduction and error analysis for the physical sciences, 2nd ed.WCB McGraw-Hill, Boston, MA, 1992.